Brain Arachidonic Acid Incorporation Is Decreased in Heart Fatty Acid Binding Protein Gene-Ablated Mice†

Eric J. Murphy,*,‡ Yuji Owada,§ Noriko Kitanaka,§ Hisatake Kondo,§ and Jan F. C. Glatz||

Department of Pharmacology, Physiology, and Therapeutics and Department of Chemistry, University of North Dakota, Grand Forks, North Dakota 58202-9037, Department of Histology, Graduate School of Medicine, Tohoku University, Sendai, Japan, and Department of Molecular Genetics, Cardiovascular Research Institute Maastricht, Maastricht, The Netherlands

Received December 23, 2004; Revised Manuscript Received March 6, 2005

ABSTRACT: Heart fatty acid binding protein (H-FABP) is expressed in neurons, but its role in brain fatty acid incorporation and metabolism is poorly defined. We examined the effect of H-FABP gene ablation on brain incorporation of arachidonic ([1-^{14}C]20:4*n*-6) or palmitic ([1-^{14}C]16:0) acid in vivo. Analysis of brain mRNA confirmed gene ablation and demonstrated no compensatory changes in the levels of other FABP mRNA in the gene-ablated mice. In brains from H-FABP gene-ablated mice, the incorporation coefficient for [1-^{14}C]20:4*n*-6 was reduced 24%, while that for [1-^{14}C]16:0 was unaffected. Within the organic and aqueous fractions, significantly more [1-^{14}C]20:4*n*-6 was distributed into the aqueous fraction, suggesting a disruption in the metabolic targeting of 20:4*n*-6 in these mice. There was less incorporation of [1-^{14}C]20:4*n*-6 into total phospholipids and a marked reduction (51%) in the level of incorporation into the choline glycerophospholipids (ChoGpl). Because FABP can influence steady-state lipid mass, brain individual lipid masses were measured. The brain total phospholipid mass was reduced 17% by gene ablation, ascribed to a 27% and 32% reduction in the masses of ChoGpl and sphingomyelin, respectively. Plasmalogen subclass masses were also reduced, suggesting that H-FABP may augment brain plasmalogen synthesis. In gene-ablated mice, the phosphatidylinositol 20:4*n*-6 level was reduced 25%, while the proportion of total *n*-6 fatty acids was reduced in the major phospholipid classes. Thus, these results demonstrate for the first time that H-FABP expression influences brain 20:4*n*-6 uptake and trafficking as well as steady-state brain lipid levels.

The physiological function of heart-type fatty acid binding protein (H-FABP)[1] in brain fatty acid uptake and subsequent metabolism is not well understood. A recently produced H-FABP gene-ablated mouse (*1*, *2*) provides a useful tool for studying this issue. H-FABP is a 15 kDa cytosolic protein found in heart, muscle, brain, and lactating mammary gland (*3*−*6*). A unique promoter region appears to account for the specific tissue localization of H-FABP expression (*7*). H-FABP binds fatty acids with a high affinity and can transport fatty acids between vesicles via a collisional mechanism involving the direct interaction between H-FABP and membrane for fatty acid binding to occur (*8*). H-FABP also demonstrates a preferential binding of the *n*-6 fatty acid family (*9*), suggesting a potential role for trafficking of arachidonic acid (20:4*n*-6). Further, H-FABP binds epoxyeicosatrienoic acids in vitro and prolongs the half-life of these molecules by preventing their hydration (*10*). H-FABP levels are reduced nearly 35% in aged mouse brain (*11*), and they are also reduced in brain regions affected by Alzheimer's disease (*12*), suggesting that H-FABP may have an important role in normal brain function. However, the role of H-FABP in brain fatty acid uptake and lipid metabolism in intact animals is poorly understood.

H-FABP gene-ablated mice demonstrate a normal phenotype with regard to fertility, sex ratio, and weight gain (*1*). These mice develop cardiac hypertrophy with increasing age (*1*) and have altered fatty acid uptake and trafficking characteristics both in vivo (*1*, *13*) and in isolated myocytes (*2*). The slower uptake of fatty acids results in a shift in heart glucose utilization (*1*, *2*), although the capacity of mitochondria for β-oxidation remains intact (*2*). In heart, there are no compensatory increases in the expression of or levels of other FABP types or of putative membrane-associated fatty acid transport proteins (*2*), although a similar effect in brain is unknown.

† This work was supported by American Heart Association Grant 0151121Z and by National Institutes of Health Grant 1R21 NS043697-01A to E.J.M. and, in part, by a grant from the Netherlands Heart Foundation to J.F.C.G. J.F.C.G. is a Netherlands Heart Foundation Professor of Cardiac Metabolism.

* To whom correspondence should be addressed: Department of Pharmacology, Physiology, and Therapeutics, School of Medicine and Health Sciences, University of North Dakota, 501 N. Columbia Rd., Room 3700, Grand Forks, ND 58202-9037. Phone: (701) 777-3450. Fax: (701) 777-4490. E-mail: emurphy@medicine.nodak.edu.

‡ University of North Dakota.

§ Tohoku University.

|| Cardiovascular Research Institute Maastricht.

[1] Abbreviations: FABP, fatty acid binding protein; I-FABP, intestinal FABP; L-FABP, liver FABP; H-FABP, heart FABP; TAGs, triacylglycerols; DAG, diacylglycerols; ChoGpl, choline glycerophospholipids; EtnGpl, ethanolamine glycerophospholipids; PtdSer, phosphatidylserine; PtdIns, phosphatidylinositol; CerPCho, sphingomyelin; PlsEtn, ethanolamine plasmalogen; PakEtn, 1-*O*-alkyl-2-acyl-glycerophosphoethanolamine; PlsCho, choline plasmalogen; PakCho, 1-*O*-alkyl-2-acyl-glycerophosphocholine; 16:0, palmitic acid; 20:4*n*-6, arachidonic acid.

10.1021/bi047292r CCC: $30.25
Published on Web 03/30/2005

The brain expresses three different members of the fatty acid binding protein family (*14*, *15*). In brain, expression of these intracellular fatty acid binding proteins is temporally and spatially distinct. Brain FABP (B-FABP) is developmentally expressed in radial glial cells (*15*, *16*) and is expressed at lower levels in adult mice (*6*, *15*). B-FABP has a preference for binding the *n*-3 fatty acid family (*6*, *17*) and may be involved in the trafficking and targeting of these fatty acids during brain development, especially to myelin (*18*). B-FABP is estimated to comprise 0.1% of the total cytosolic protein in adult brain (*6*). Epidermal FABP (E-FABP) is expressed in the adult animal but is expressed primarily in gray matter in glial cells, although there does appear to be some expression in white matter as well (*15*). H-FABP has repeatedly been identified in the brain (*5*, *6*, *15*, *19*) and is expressed in neurons with the highest level of expression in cortical layers, in the hippocampus, and in the dentate gyrus (*15*, *19*). H-FABP is estimated to comprise 0.01% of the total cytosolic protein in adult brain (*6*). Because H-FABP has a binding preference for *n*-6 fatty acids (*9*), it suggests that this protein may be involved in neuronal 20:4*n*-6 uptake and trafficking.

While FABPs facilitate fatty acid uptake, FABP expression is also associated with an increase in phospholipid mass and alterations in phospholipid acyl chain composition (*20*, *21*). Liver FABP (L-FABP) expression and intestinal FABP (I-FABP) expression increase the basal total phospholipid mass 1.7- and 1.3-fold in L-cell fibroblasts, respectively (*20*, *21*). This is consistent with the observed capacity for FABP to enhance phosphatidic acid biosynthesis in vitro (*22*−*24*). I-FABP expression and L-FABP expression increase the mass of individual phospholipid classes as well as the mass of the plasmalogen subclasses of the ethanolamine and choline glycerophospholipids (*20*). Similarly, in hearts from H-FABP gene-ablated mice, the individual phospholipid class mass, including the plasmalogens, is altered (*13*), suggesting FABP expression impacts phospholipid metabolism in vivo. Further, I-FABP expression and L-FABP expression increase the degree of unsaturation in phospholipid acyl chain composition in L-cell fibroblasts (*20*). In hearts from H-FABP gene-ablated mice, there is a derangement of 20:4*n*-6 targeting, as these levels are decreased in heart phospholipids (*13*). Hence, FABP expression alters steady-state phospholipid mass and acyl chain composition, suggesting a role in cellular lipid metabolism beyond facilitation of fatty acid incorporation. A similar function of H-FABP in the brain is unknown.

To better address the potential role of H-FABP in brain fatty acid incorporation and trafficking, gene-ablated mice were infused with either [1-^{14}C]16:0 or [1-^{14}C]20:4*n*-6 (170 μCi/kg) and brain fatty acid incorporation and disposition were assessed using standard lipid analytical techniques. The effects of H-FABP deletion on steady-state phospholipid mass and phospholipid acyl chain composition were also addressed. In addition, using RT-PCR, we demonstrate no compensatory changes in other FABPs found in the brain. Our results show a differential effect of H-FABP on fatty acid incorporation, with deletion decreasing 20:4*n*-6 incorporation, indicative of a previously unknown role for H-FABP in brain fatty acid uptake. Furthermore, H-FABP was important in the trafficking of 20:4*n*-6 to cellular lipid pools, consistent with the decrease in phosphatidylinositol 20:4*n*-6 levels in gene-ablated mice, suggesting that H-FABP has a role in directing 20:4*n*-6 to specific phospholipid classes.

EXPERIMENTAL PROCEDURES

Animals. Male mice (25−30 g) were obtained from the Cardiovascular Research Institute Maastricht and were maintained on standard laboratory chow diet and water ad libitum. Prior to surgery and infusion, the mice were fasted overnight prior to the morning of surgery, with infusion occurring 3−4 h post-operative. Mice in both groups were 9−15 months old, and there were no correlations between age and any of the lipid parameters measured in either group. This study was conducted in accordance with the National Institutes of Health Guidelines for the Care and Use of Laboratory Animals (NIH Publication 80-23) and under an animal protocol approved by the IACUC at the University of North Dakota (Protocol 0110-1).

Mouse Surgery. After the mice were anesthetized with halothane (1−3%), their femoral artery and vein were catheterized with polyethylene tubing (PE-10). The wound area was anesthetized with xylocaine (1%) and closed using standard surgical staples. The hindquarters of the mouse was immobilized by taping the hind legs and hindquarters to a wooden block, and the mice were maintained post-operatively in a temperature-controlled environment for 3−4 h.

Tracer Preparation. [1-^{14}C]16:0 and [1-^{14}C]20:4*n*-6 were synthesized by Moravek Biochemical (Brea, CA). The radiotracer was prepared by taking an aliquot of the tracer in ethanol and evaporating the ethanol under a constant stream of N_2 at 50 °C. Prior to use, radiotracer purity was assessed by gas−liquid chromatography and was found to be >97%. The fatty acid tracer was solubilized in 5 mM HEPES (pH 7.4) buffer containing "essentially fatty acid free" bovine serum albumin (50 mg/mL, Sigma Chemical Co., St. Louis, MO). Solubilization was facilitated by sonication in a bath sonicator for 45 min at 45 °C. The appropriate amount of radiotracer was prepared for each mouse using the mouse's weight based upon the infusion parameters of 170 μCi/kg (*25*).

Infusion (intravenous). Awake, fasted, adult male mice were infused with 170 μCi/kg of either [1-^{14}C]16:0 or [1-^{14}C]-20:4*n*-6 into the femoral vein over the course of 10 min at a constant rate of 30 μL/min to achieve steady-state plasma radioactivity. Prior to and during the experimental period, arterial blood samples (∼20 μL) were taken to determine plasma radioactivity. Following infusion, each mouse was killed using pentobarbital (100 mg/kg, intravenous). Its brain was rapidly removed and frozen in liquid nitrogen. The time from pentobarbital injection to freezing was 25 ± 5 s. All tissue was stored at −80 °C until it was used.

Plasma Extraction. Arterial blood samples, taken at fixed times during the infusion period, were stored for up to 10 min on ice before the plasma was separated by centrifugation with a Beckman (Fullerton, CA) microfuge. Plasma lipids were then extracted by transferring a 10 μL aliquot of plasma into a tube containing 2 mL of chloroform and methanol (2:1, v/v) and then mixing it by vortexing (*26*). The addition of 0.4 mL of 0.9% KCl to these tubes resulted in two phases. These phases were thoroughly mixed and then separated

overnight in a −20 °C freezer. The upper phase was removed, and the lipid-containing lower phase was rinsed with 0.43 mL of the theoretical upper phase to remove any aqueous soluble contaminants (*26*). The radioactivity in the upper phase was determined using a Beckman LS5000 CE liquid scintillation counter. Lower phase radioactivity was assessed in a portion of the lower phase using a Beckman LS5000 CE liquid scintillation counter.

Blood Extraction. Following the procedure described above for plasma, whole blood was extracted to correct for radioactivity contributed by residual blood left in the tissue. For the brain, the level of residual blood left in the brain tissue was estimated to be 2% (*27*−*29*).

Tissue Lipid Extraction. Frozen brain tissue was pulverized at liquid nitrogen temperatures. Lipids from brain tissue powder were extracted in a Tenbroeck tissue homogenizer using a two-phase system (*26*). Briefly, the tissue mass (grams) was multiplied by a correction factor of 1.28 to convert it to an equivalent value expressed in milliliters (*30*). This value represents 1 volume. The pulverized tissue was placed in the homogenizer, and 17 volumes of chloroform and methanol (2:1, v/v) was added. Tissue was homogenized until there was a fine particulate-like powder. The solvent was removed and the homogenizer rinsed with 3 volumes of chloroform and methanol (2:1, v/v). The rinse was added to the original sample, and 4 volumes of a 0.9% KCl solution was added to this combined lipid extract. After vigorous mixing, phase separation was facilitated by centrifugation as described above. The upper phase and proteinaceous interface were removed and saved in a 20 mL glass scintillation vial. The lower organic phase was washed twice with 2 mL of theoretical upper phase, with phase separation facilitated by centrifugation between washes. The washes were removed and combined with the previously removed upper phase. The washed lower phase was dried under a stream of nitrogen, and the lipids were redissolved in 1 mL of *n*-hexane and 2-propanol (3:2, v/v) containing 5.5% H_2O.

Aqueous Fraction. The radioactivity in the aqueous fraction from the brain tissue extraction, including the theoretical upper phase from the two wash steps, was measured using liquid scintillation counting. Radioactivity was determined after addition of 10 mL of Scintiverse II BD (Fisher Scientific, Pittsburgh, PA) using a Beckman LS5000 CE liquid scintillation counter. The addition of the aqueous material to the scintillation cocktail did not adversely affect the counter efficiency.

Thin Layer Chromatography. Phospholipids and neutral lipids were separated by thin-layer chromatography (TLC). For each separation, 100 μL of sample was spotted onto a TLC plate. Phospholipids were separated on heat-activated Whatman silica gel-60 plates (20 cm × 20 cm, 250 μm) and developed in a chloroform/methanol/acetic acid/water mixture (50:37.5:3.5:2 by volume) (*24*). This method separates all major phospholipids. Neutral lipids were separated on heat-activated Whatman silica gel-60 plates (20 cm × 20 cm, 250 μm) and developed in a petroleum ether/diethyl ether/acetic acid mixture (75:25:1.3 by volume) (*31*). This solvent system resolves cholesteryl esters, diacylglycerols, nonesterified fatty acids, and triacylglycerols. Lipid fractions are identified using authentic standards (Doosan-Serday, Englewood Cliffs, NJ, and NuChek Prep, Elysian, MN).

Mass of Individual Lipid Classes. Phospholipid mass was determined by assaying the lipid phosphorus content of individual lipid classes separated by TLC as described above (*32*). Cholesterol mass was assayed using an iron binding assay after separation by TLC as described above (*33*).

Plasmalogen Mass. The plasmalogen mass was determined following separation of individual phospholipid classes in the brain lipid extracts by high-performance liquid chromatography (HPLC) (*34*). One-half of the choline glycerophospholipid (ChoGpl) and of the ethanolamine glycerophospholipid (EtnGpl) fractions were dried under nitrogen and subjected to mild acidic hydrolysis followed by separation using HPLC (*35*). The proportion of plasmalogen in this separation was used to calculate plasmalogen mass using the EtnGpl and ChoGpl masses determined by TLC as reported above.

Phospholipid Acyl Chain Composition. The fatty acid composition of the PtdIns, phosphatidylserine (PtdSer), ChoGpl, and EtnGpl was determined following transesterification in 0.5 M KOH in methanol to form the fatty acid methyl ester (*36*). Individual fatty acids were separated by gas−liquid chromatography (GLC) using an SP-2330 column [0.32 mm (inside diameter) × 30 m (length)] and a Trace GLC system (ThermoElectron, Austin, TX) equipped with dual autosamplers and dual flame ionization detectors (FID). Fatty acids were quantified using a standard curve from commercially purchased standards (NuChek Prep), and 17:0 was the internal standard.

Liquid Scintillation Counting. Bands corresponding to the appropriate lipid fractions were scraped into 20 mL liquid scintillation vials, and 0.5 mL of H_2O was added followed by 10 mL of Scintiverse BD (Fisher Scientific). After being mixed, the samples were quantified by liquid scintillation counting at least 1 h after the addition of the liquid scintillation cocktail.

Calculations. Integrated areas for the plasma radioactivity curves were determined using the trapezoidal method (Sigma Plot, Jandel Scientific, San Rafael, CA). Total radioactivity for each individual brain fraction was normalized to the wet weight (grams wet weight) and divided by the integrated area of plasma radioactivity. This calculation essentially normalizes tissue radioactivity to the exposure of plasma tracer. The resulting coefficient is termed the unilateral incorporation coefficient or k^*, with values expressed in inverse seconds. Hence, k^* represents the radioactivity of each fraction normalized to the amount of radioactivity in the plasma to which the tissue was exposed. The following equation was used to calculate the unilateral incorporation coefficient:

$$k^* = c^*_{\text{tissue}} / \int_0^T c^*_{\text{plasma}}\, \mathrm{d}t \qquad (1)$$

where k^* is the coefficient for incorporation of tracer into a brain compartment, c^*_{tissue} is the tracer radioactivity in the brain compartment, c^*_{plasma} is the tracer radioactivity in the plasma, and T is the time of tissue sampling.

RNA Isolation and Semiquantitative RT-PCR. Tissues were isolated from wild-type and H-FABP mutant mice (10-week-old male mice, $n = 3$ for each genotype) and were immediately frozen in liquid nitrogen. Total RNA was isolated using the guanidine isothiocyanate-based TRIzol solution (GIBCO-BRL, Burlington, ON) according to the

manufacturer's instructions. First-strand cDNA was synthesized using a Reverse Transcription System (Promega, Madison, WI). RT-PCR was performed to assess gene expression of A-, B-, E-, and H-FABP mRNA in wild-type and H-FABP gene-ablated brains. Primers with the following oligonucleotide sequences were used: A-FABP, 5′-TCAACCTGGAAGACAGCTCCT-3′ and 5′-TCGACTTTCCATCCCACTTC-3′ (GenBank accession number NM_024406); B-FABP, 5′-GGGTAAGACCCGAGTTCCTC-3′ and 5′-GAGCTTGTCTCCATCCAACC-3′ (GenBank accession number BC055280); E-FABP, 5′-CAAACCGAGAGCACAGTGA-3′ and 5′-TTTGACCGCTCACTGAATTG-3′ (GenBank accession number BC002008); H-FABP, 5′-CATGAAGTCACTCGGTGTGG-3′ and 5′-TGCCATGAGTGAGAGTCAGG-3′ (GenBank accession number BC002082); β-actin, 5′-CAGGAGATGGCCACTGCCGCA-3′ and 5′-CTCCTTCTGCATCCTGTCAGCA-3′ (GenBank accession number NM_007393).

Polymerase chain reaction was carried out with a GeneAmp PCR system 9700 (Applied Biosystems, Foster, CA) using 100 ng of cDNA, 5 pmol of each oligonucleotide primer, 200 μM dNTP, 1 unit of Taq polymerase (Takara, Tokyo, Japan), and 1× PCR buffer (Takara). The PCR program was initially started with 94 °C denaturation for 4 min followed by 25 cycles of 94 °C for 1 min, 60 °C for 1 min, and 72 °C for 1 min. Linear amplification of the band was confirmed in advance for each target gene in the brain except for A-FABP under these conditions. PCR products were electrophoresed on a 1.5% agarose gel, and gel images were digitally captured by ChemiDoc XRS (Bio-Rad Laboratories, Hercules, CA), and the density of the amplified band was measured by Quantity One software (Bio-Rad Laboratories). The values were presented as a ratio of specified gene signal density divided by that of β-actin.

Statistics. Statistical analysis was done using Instat2 from GraphPad (San Diego, CA). Statistical significance was assessed using an unpaired, two-way, Student's *t* test, with a $p < 0.05$ considered to be statistically significant.

RESULTS

FABP mRNA Levels. No significant differences in B-, E-, and A-FABP expression were detected in brains from wild-type and H-FABP gene-ablated mice (Figure 1). Further, the ablation of the mRNA for H-FABP was confirmed in brains and hearts of gene-ablated mice.

Plasma Curves. The plasma curves for [1-^{14}C]16:0- and [1-^{14}C]20:4*n*-6-infused mice reached a steady state between 2 and 4 min following the start of infusion (data not shown). For [1-^{14}C]16:0-infused mice, the average integrated plasma curve area was significantly different between groups ($p < 0.05$), with values of 943 ± 61 and 1172 ± 127 nCi min^{-1} mL^{-1} for control and gene-ablated mice, respectively. For [1-^{14}C]20:4*n*-6-infused mice, the average integrated plasma curve area was 1457 ± 484 and 1420 ± 286 nCi min^{-1} mL^{-1} for control and gene-ablated mice, respectively.

Brain Fatty Acid Uptake. Brain radiotracer uptake was normalized to the integrated area under the curve and expressed as the incorporation coefficient, *k**. For [1-^{14}C]-16:0-infused mice, there were no significant differences between groups in the incorporation of tracer (Figure 2). For [1-^{14}C]20:4*n*-6-infused mice, the level of total incorporation

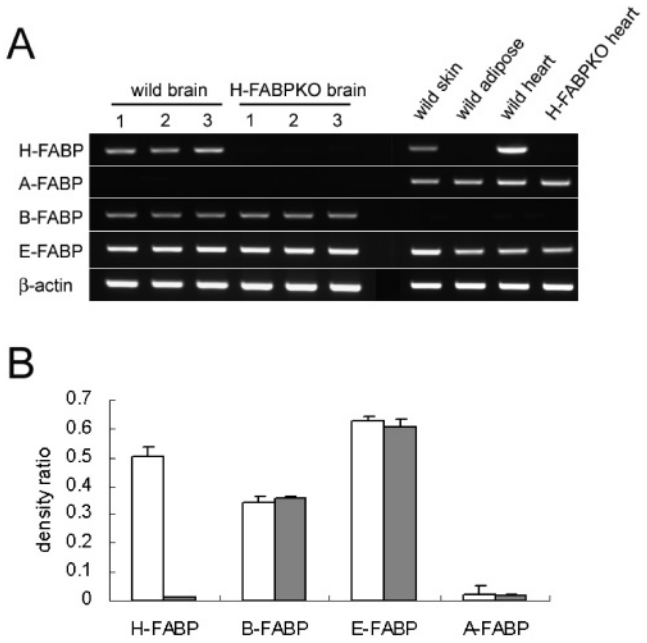

FIGURE 1: RT-PCR of brain mRNA isolated from wild-type and H-FABP gene-ablated (KO) mice ($n = 3$). For all FABPs except A-FABP, the expansion of brain mRNA and quantitation was linear between groups. Positive control tissues were obtained from wild-type mice and were skin, adipose, and heart. Note that H-FABP mRNA was absent from both heart and brain. Panel A is the gel demonstrating the reductions in the level of tissue H-FABP mRNA in the KO mice. Panel B shows the densiometric data for a group of three mice where the values represent means ± the standard deviation.

was reduced 24%, while the level of incorporation into the organic fraction was reduced 30% in the gene-ablated mice. The percent of radiotracer in the plasma extracted by the brain was calculated, and there were no differences for [1-^{14}C]16:0-infused mice. In [1-^{14}C]20:4*n*-6-infused mice, 0.80 ± 0.11% of the tracer was extracted by the brain from plasma in control mice, while 0.61 ± 0.11% was extracted from the plasma of gene-ablated mice. Thus, two different measures of fatty acid uptake demonstrate a significant reduction (~25%) in the level of incorporation of 20:4*n*-6 into the brains of H-FABP gene-ablated mice.

Distribution of Fatty Acids into Metabolic Compartments. The effects of H-FABP gene ablation on the distribution of fatty acids into the aqueous and organic fractions were determined (Figure 3). For [1-^{14}C]16:0-infused mice, there was no change in tracer distribution. In [1-^{14}C]20:4*n*-6-infused mice, 1.3-fold more tracer was targeted to the aqueous fraction and 17% less tracer was targeted to the organic fraction.

Targeting of Fatty Acids to Esterified Lipid Compartments. The esterification of tracers into either the neutral lipid fraction or into the phospholipid fraction was also assessed (Figure 4). There were no differences between groups in the incorporation or the distribution of [1-^{14}C]16:0 into the neutral lipids or phospholipids (Figure 3A,B). In [1-^{14}C]20:4*n*-6-infused mice, there was a 38% reduction in the level of incorporation of tracer into phospholipids, while the incorporation into neutral lipids was unaffected (Figure 4A). However, there was no net change in the distribution of tracer among the esterified neutral lipids and phospholipids (Figure 4B). Thus, H-FABP gene deletion resulted in a selective

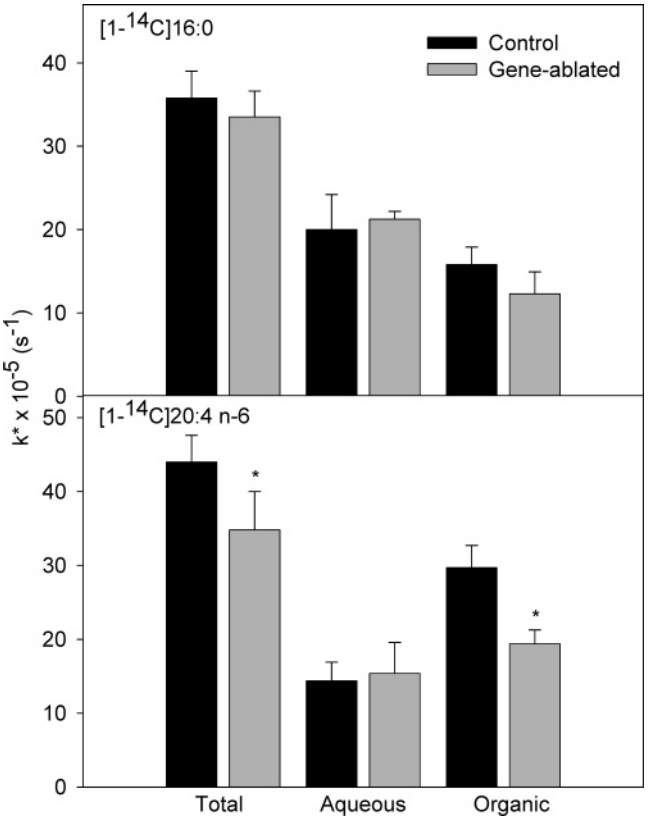

FIGURE 2: Incorporation of [1-^{14}C]16:0 or [1-^{14}C]20:4*n*-6 into brain tissue from control (filled bars) and H-FABP gene-ablated (empty bars) mice expressed as the level of total incorporation or incorporation into the aqueous and organic fractions. All values are expressed as k^* (s^{-1}) and were corrected for radioactivity associated with the residual blood left in the brain tissue. Values represent means ± the standard deviation ($n = 4-5$). The asterisk indicates statistical significance from control mice ($p < 0.05$).

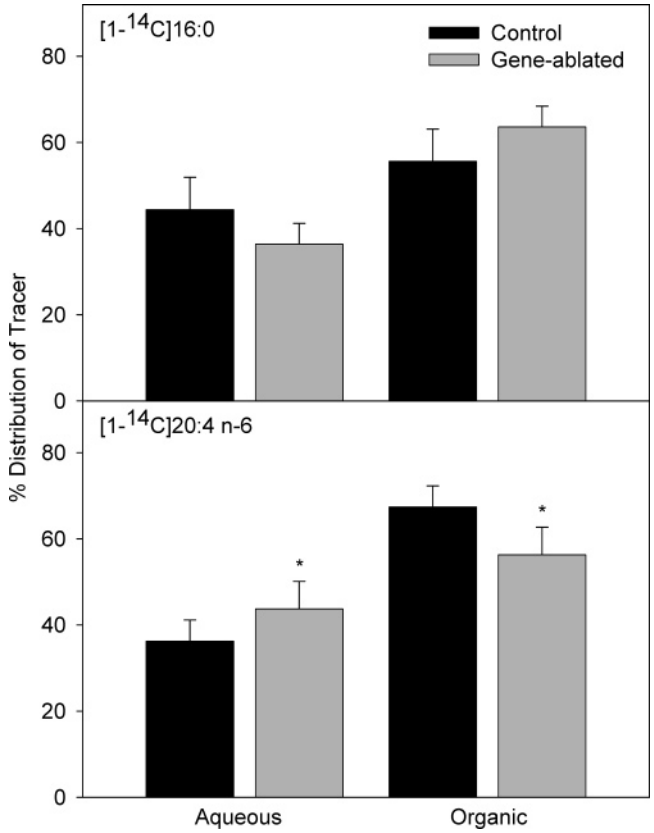

FIGURE 3: Distribution of [1-^{14}C]16:0 and [1-^{14}C]20:4*n*-6 in brain aqueous and organic fractions from control (filled bars) and H-FABP gene-ablated (empty bars) mice. Values represent means ± the standard deviation ($n = 4-5$). The asterisk indicates statistical significance from control mice ($p < 0.05$).

decrease in the level of incorporation of fatty acids into the phospholipid compartment, yet H-FABP expression did not alter the targeting of tracer to these two pools.

Targeting of Fatty Acid to Individual Lipid Classes. The effect of H-FABP gene ablation on incorporation of fatty acids into individual lipid classes was also determined (Table 1). There were no alterations in incorporation of or targeting of [1-^{14}C]16:0 (Table 1, top and bottom). In [1-^{14}C]20:4*n*-6-infused mice, the level of incorporation of tracer into the ChoGpl was reduced 51% in gene-ablated mice (Table 1, top). This reduction in the level of incorporation was also reflected in a 22% reduction in the extent of targeting to ChoGpl (Table 1, bottom).

Because plasmalogens in brain are a large reservoir of 20:4*n*-6, we also examined the incorporation of [1-^{14}C]20:4*n*-6 into this compartment. There was no alteration in the incorporation into the plasmalogen subclasses, with the only significant reduction limited to the acid stable fraction of the ChoGpl comprised primarily of phosphatidylcholine (data not shown). Thus, H-FABP gene ablation caused a significant decrease in the level of incorporation of [1-^{14}C]20:4*n*-6 into the ChoGpl, without affecting incorporation into the ether lipid subclasses.

Brain Steady-State Phospholipid Mass. Brain phospholipid mass and composition were also assessed in H-FABP gene-ablated and control mice (Table 2). The total phospholipid mass was significantly reduced 17% in gene-ablated mice, with values of 42 983 ± 2903 nmol/g wet weight in control mice and 35 543 ± 2084 nmol/g wet weight in gene-ablated mice. The masses of phosphatidic acid (PtdOH) and of phosphatidylglycerol (PtdGro) were increased 2.6- and 2.2-fold in gene-ablated mice, respectively. The mass of choline-containing phospholipids was also reduced, with a 27 and a 32% reduction in ChoGpl and sphingomyelin (CerPCho) mass, respectively, in gene-ablated mice. These changes in steady-state mass were also demonstrated by the corresponding increase in the percent mole composition for PtdGro and PtdOH, with a reduction in the percent mole composition for ChoGpl and CerPCho. Hence, H-FABP gene ablation significantly altered steady-state phospholipid mass, suggesting that H-FABP has a role in maintaining phospholipid biosynthesis.

Because FABP expression can influence plasmalogen mass (*13*, *20*), we also examined the effect of gene ablation on brain plasmalogen mass (Table 3). Unlike targeting of [1-^{14}C]-20:4*n*-6 to the plasmalogen subclasses, steady-state plasmalogen mass was significantly altered by H-FABP gene ablation. The mass of the ethanolamine plasmalogen (PlsEtn) was significantly reduced 13%, while that of the choline plasmalogen (PlsCho) was reduced 57% in gene-ablated as compared to control mice. The PlsEtn:PlsCho ratio was increased in gene-ablated mice, from 5.1 ± 0.7 for control to 10.6 ± 1.8 for gene-ablated mice. Thus, H-FABP expression affects brain plasmalogen steady-state mass in the absence of targeting 20:4*n*-6 to the plasmalogens.

Brain Cholesterol Mass. The cholesterol mass and cholesterol:phospholipid ratio were also determined for each

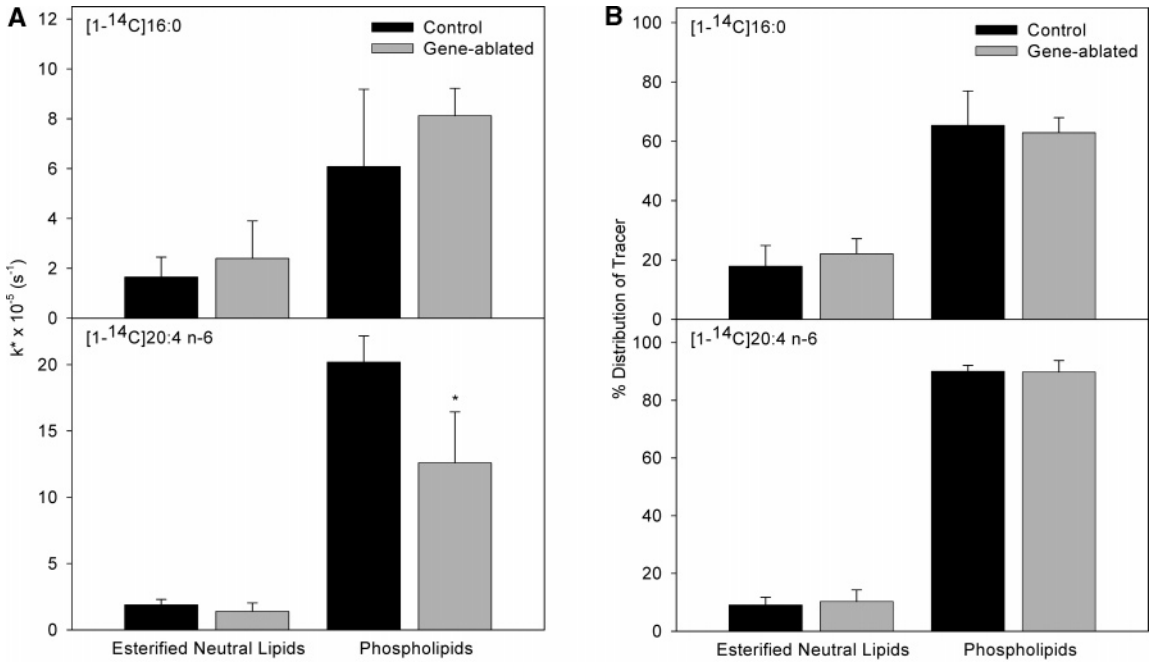

FIGURE 4: Incorporation of tracer (A) and distribution of tracer (B) in the esterified neutral lipids and phospholipids of control (filled bars) and H-FABP gene-ablated (empty bars) mice. All values are expressed as k^* (s^{-1}) and were corrected for radioactivity associated with the residual blood left in the brain tissue. The distribution was determined based upon k^* values found in panel A. Values represent means ± the standard deviation ($n = 4-5$). The asterisk indicates statistical significance from control mice ($p < 0.05$).

Table 1: H-FABP Expression Increases the Level of 20:4*n*-6 Targeting to Choline Glycerophospholipids[a]

	[1-^{14}C]16:0				[1-^{14}C]20:4*n*-6			
	control		gene-ablated		control		gene-ablated	
class	mean	SD	mean	SD	mean	SD	mean	SD
	k^* ($\times 10^{-5}$ s^{-1})							
DAG	1.1	1.0	1.1	0.9	1.2	0.7	0.7	0.4
EtnGpl	0.8	0.6	0.9	0.4	2.0	0.6	1.0	0.7
PtdIns	0.4	0.4	0.1	0.1	6.4	1.9	5.2	2.2
PtdSer	0.0	0.0	0.1	0.2	1.2	0.6	0.8	0.9
ChoGpl	4.5	0.9	4.9	0.6	9.2	1.6	4.5	1.9[b]
CerPCho	0.3	0.5	1.3	0.4	0.6	0.4	0.6	0.8
	$n = 4$		$n = 5$		$n = 4$		$n = 5$	
	(B) % Distribution							
DAG	10.5	10.1	8.0	7.1	5.4	3.4	4.9	2.1
EtnGpl	7.4	5.3	6.6	4.5	9.2	2.9	7.9	5.6
PtdIns	3.6	3.9	0.5	1.2	28.5	7.0	36.1	7.8
PtdSer	0.0	0.0	1.1	1.3	5.2	2.8	5.9	6.1
ChoGpl	50.2	8.5	40.9	6.5	40.9	5.6	31.8	5.2[b]
CerPCho	3.4	4.6	11.4	3.6	3.0	2.0	4.5	4.6
	$n = 4$		$n = 5$		$n = 4$		$n = 5$	

[a] Values represent the mean ± the standard deviation ($n = 4-5$). The distribution of k^* was determined using the values in the top portion of the table. [b] Significantly different from the control group value ($p < 0.05$).

Table 2: H-FABP Expression Alters Brain Steady-State Phospholipid Mass and Composition[a]

	mass (nmol/g wet weight)				composition (mol %)			
	control		gene-ablated		control		gene-ablated	
	mean	SD	mean	SD	mean	SD	mean	SD
Ptd_2Gro	871	287	710	171	2.0	0.6	2.0	0.4
PtdGro	253	130	562	114[b]	1.0	1.2	1.6	0.3
PtdOH	245	132	626	240[b]	0.5	0.3	1.7	0.6[b]
EtnGpl	13329	1441	12161	779	31.0	2.9	34.1	2.5[b]
PtdIns	1421	219	1330	210	3.3	0.5	3.7	0.5
PtdSer	4225	584	3869	441	9.6	0.9	10.8	1.0
ChoGpl	17891	1461	13026	1023[b]	41.5	1.9	36.5	2.6[b]
CerPCho	4802	599	3260	816[b]	11.1	1.1	9.5	1.4[b]
	$n = 9$		$n = 7$		$n = 9$		$n = 7$	

[a] Values represent the mean ± the standard deviation ($n = 5-6$). [b] Significantly different from the control group value ($p < 0.05$).

Table 3: H-FABP Expression Increases Brain Steady-State Plasmalogen Mass[a]

	mass (nmol/g wet weight)				% Gpl class (mol %)			
	control		gene-ablated		control		gene-ablated	
	mean	SD	mean	SD	mean	SD	mean	SD
PakEtn and PtdEtn	7021	843	6538	421	52.2	1.2	53.8	2.5
PlsEtn	6430	675	5622	540[b]	47.8	1.2	46.2	2.5
PakCho and PtdCho	16043	689	12265	908[b]	92.7	1.1	95.8	0.8[b]
PlsCho	1267	174	551	72[b]	7.3	1.1	4.2	0.8[b]
	$n = 9$		$n = 7$		$n = 9$		$n = 7$	

[a] Values represent the mean ± the standard deviation ($n = 7-9$). [b] Significantly different from the control group value ($p < 0.05$).

group. The level of brain cholesterol was significantly ($p < 0.05$) reduced 24% in brains from gene-ablated mice compared to control. The cholesterol mass was 26 827 ± 1595 nmol/g wet weight in control mice and 20 341 ± 1384 nmol/g wet weight in gene-ablated mice. The brain cholesterol:phospholipid ratio was 0.619 ± 0.038 in control mice and 0.566 ± 0.059 in gene-ablated mice. However, because of a net reduction in total phospholipid mass, the cholesterol:phospholipid ratio was not different between groups.

Brain Phospholipid Acyl Chain Composition. Acyl chain compositions were determined for ChoGpl, EtnGpl, PtdSer, and PtdIns (Table 4). For ChoGpl, the level of total *n*-6 fatty acids was decreased 20% in the gene-ablated mice and the *n*-3/*n*-6 ratio was increased 1.2-fold, although there was no net change in 22:6*n*-3 or 20:4*n*-6 proportions. Similarly, in EtnGpl, the total level of *n*-6 fatty acids was decreased 11%, but there was no change in the 20:4*n*-6 or 22:6*n*-3 levels. For PtdSer, the level of total *n*-6 fatty acids was decreased 13%, but there was no net change in 20:4*n*-6 or 22:6*n*-3.

Table 4: H-FABP Expression Alters Brain Phospholipid Fatty Acid Composition[a]

	ChoGpl				EtnGpl				PtdSer				PtdIns			
	control		gene-ablated		control		gene-ablated		control		gene-ablated		control		gene-ablated	
fatty acid	mean	SD	mean	SD	mean	SD	mean	SD	mean	SD	mean	SD	mean	SD	mean	SD
16:0	32.0	2.3	34.0	3.8	4.4	0.3	4.7	0.9	3.0	1.0	2.3	0.6	9.8	0.8	4.9	0.9[b]
18:0	17.6	0.5	17.0	1.0	23.0	1.0	22.3	0.6	42.2	1.0	40.8	0.8[b]	33.6	0.5	32.8	0.7
18:1*n*-9	22.9	1.0	24.4	1.1	12.4	1.8	15.1	0.7[b]	16.8	2.2	18.2	1.3	6.3	0.8	12.4	0.5[b]
18:1*n*-12	8.4	0.2	8.0	0.3	3.0	0.6	3.3	0.5	2.4	0.3	2.5	0.2	3.9	0.2	4.1	0.2
18:2*n*-6	0.8	0.1	0.9	0.1	ND[c]		ND[c]		0.7	0.7	ND[c]		ND[c]		ND[c]	
20:1*n*-9	1.5	0.2	1.4	0.1	3.3	1.2	4.7	0.6	1.3	0.3	1.6	0.2	ND[c]		2.5	0.4
20:3*n*-6	1.1	0.4	0.5	0.1[b]	1.9	1.3	ND[c]		0.5	0.1	0.4	0.0	ND[c]		ND[c]	
20:4*n*-6	7.7	0.7	6.7	0.7	15.3	1.2	14.7	0.3	5.8	0.5	5.2	0.6	40.5	1.3	30.3	0.2[b]
22:4*n*-6	ND[c]		ND[c]		5.1	0.1	5.0	0.1	2.1	0.1	2.1	0.1	2.4	1.8	1.8	0.7
22:5*n*-3	ND[c]		ND[c]		ND[c]		ND[c]		0.5	0.4	1.0	0.8	ND[c]		ND[c]	
22:6*n*-3	7.2	0.6	7.0	0.8	31.6	1.8	30.4	1.4	24.7	2.6	25.7	1.5	3.5	0.1	8.5	1.6[b]
sat	49.6	1.9	51.0	2.8	27.4	1.1	26.9	1.4	45.2	0.6	43.2	0.9	43.4	1.0	37.7	0.9[b]
unsat	50.4	1.9	49.0	2.8	72.6	1.1	73.1	1.4	54.8	0.6	56.8	0.9	56.6	1.0	62.3	0.9[b]
MUFA	32.7	1.1	33.8	1.5	18.7	3.5	22.9	1.9[b]	20.5	2.5	22.3	1.5	10.2	1.0	18.9	0.9[b]
PUFA	17.6	1.3	15.2	1.4[b]	53.9	2.5	50.2	1.4	34.4	2.7	34.6	2.3	46.4	1.7	43.4	1.4[b]
n-3	7.7	0.6	7.2	0.8	31.6	1.8	30.4	1.4	25.2	2.9	26.7	1.8	3.5	0.1	8.7	1.7[b]
n-6	10.0	1.1	7.9	1.0[b]	22.3	1.4	19.8	0.3[b]	9.1	0.6	7.9	0.7[b]	42.9	1.7	34.7	0.7[b]
n-3/*n*-6	0.77	0.09	0.91	0.05[b]	1.42	0.11	1.54	0.08	2.79	0.45	3.40	0.23[b]	0.09	0.01	0.25	0.05[b]
unsat/sat	1.02	0.07	0.96	0.10	2.66	0.15	2.72	0.19	1.21	0.03	1.32	0.05[b]	1.30	0.05	1.66	0.07[b]
PUFA/MUFA	0.54	0.04	0.45	0.03[b]	2.97	0.56	2.21	0.22[b]	1.71	0.31	1.56	0.21	4.62	0.60	2.29	0.17[b]
MUFA/sat	0.66	0.04	0.67	0.07	0.69	0.16	0.86	0.11	0.45	0.05	0.52	0.03[b]	0.24	0.02	0.50	0.02[b]
PUFA/sat	0.36	0.04	0.30	0.04[b]	1.97	0.04	1.87	0.11	0.76	0.06	0.80	0.07	1.06	0.07	1.15	0.06
	$n = 5$		$n = 5$		$n = 5$		$n = 5$		$n = 5$		$n = 5$		$n = 5$		$n = 4$	

[a] Values represent the mean ± the standard deviation ($n = 4-5$). [b] Significantly different from the control group value ($p < 0.05$). [c] Not detected.

However, in PtdIns, the levels of 20:4*n*-6 were reduced 25% accompanied by a 2.4-fold increase in the level of 22:6*n*-3 in gene-ablated mice. This phospholipid class demonstrated a number of important changes in acyl chain composition, including more oleic acid (18:1*n*-9) and less 16:0, causing a shift in a majority of the fatty acid indices. For instance, the *n*-3:*n*-6 ratio was increased 2.8-fold, indicating a dramatic shift in the amount of 20:4*n*-6 and 22:6*n*-3 in PtdIns. Thus, although the *n*-6 fatty acid index was decreased in all of the major phospholipid classes, the greatest magnitude of changes was found in PtdIns.

DISCUSSION

Fatty acids are rapidly taken up by the brain and esterified into stable lipid compartments; however, the role of proteins in facilitating this process is poorly understood. Both transporters localized in the plasma membrane (*37*−*42*) and FABP localized in the cytosol (*1*, *2*, *13*) may facilitate this process in the brain as well as other organ systems. Although the role of membrane-localized transporters in brain fatty acid uptake is unknown, in heart CD-36 is involved in facilitating myocardial fatty acid uptake, and inhibition of this transporter inhibits cellular fatty acid uptake (*37*, *40*, *41*). Similarly, H-FABP expression in heart stimulates fatty acid uptake in isolated heart myocytes (*1*, *2*) and in intact mice (*1*, *13*). Although the brain expresses three different FABPs (*14*), the role of these proteins in brain fatty acid uptake and subsequent metabolism, including esterification into stable lipid compartments, is unknown. To address this issue, we infused H-FABP gene-ablated and control mice with either [1-^{14}C]16:0 or [1-^{14}C]20:4*n*-6 and quantified incorporation and disposition of brain fatty acids into stable lipid compartments. Further, because FABP expression can impact steady-state phospholipid mass (*13*, *20*, *21*), we determined the impact of H-FABP expression on brain steady-state phospholipid mass and acyl chain composition.

In A-FABP gene-ablated mice, adipocyte E-FABP expression is enhanced, thus partially compensating for the reduction in the level of A-FABP (*43*). A similar compensation could occur in the brains of H-FABP gene-ablated mice. However, because FABPs are temporally and spatially expressed in different cell types in the brain (*14*, *15*), the existence of a similar compensatory mechanism is less likely. This was confirmed using PCR to quantify mRNA from total brain. Our results demonstrate no compensatory increase in the level of FABP expression in brains from H-FABP gene-ablated mice.

In heart, H-FABP facilitates the incorporation of both 16:0 and 20:4*n*-6, but differentially affects targeting of these fatty acids to heart lipid compartments (*13*). However, in brain there was a differential effect at the level of fatty acid uptake, with a reduction in the level of total 20:4*n*-6 incorporation in the absence of any alteration in 16:0 incorporation (Figure 2). This is consistent with the observation that H-FABP has a preference for binding of the *n*-6 fatty acid family (*9*). However, the striking difference between 16:0 and 20:4*n*-6 incorporation demonstrates a means by which the brain may selectively take up fatty acids with greater biological significance, such as 20:4*n*-6 for use by neurons, which account for ~10% of the cells found in brain (*44*). In this light, the impact of H-FABP expression on this process is considerably greater than the 25% reduction in the level of incorporation may imply.

In cell expression systems, FABP expression stimulates fatty acid uptake nearly 1.7-fold (*45*−*48*), but the enhancement in uptake is dependent upon the type of FABP (*46*, *47*). Nonetheless, in these systems, FABP expression enhances incorporation to an extent similar to the decrease in the level of incorporation observed in the H-FABP gene-

ablated mice (*1*, *13*) and in myocytes isolated from these mice (*1*, *2*). However, in none of these systems was there an observable selectivity for fatty acid uptake like that observed in the brains of H-FABP gene-ablated mice, suggesting that the brain may use H-FABP to selectively acquire and traffic 20:4*n*-6.

With regard to trafficking of these two fatty acids in the brain, 16:0 was unaffected by H-FABP expression, while 20:4*n*-6 was affected. In the absence of H-FABP expression, more 20:4*n*-6 was targeted to the aqueous fraction (Figure 3), indicating a greater use of 20:4*n*-6 for β-oxidation in the brain, presumably for acquisition of carbon units for biosynthesis of other molecules such as neurotransmitters (*49*, *50*). More importantly, H-FABP expression appears to be key for directing 20:4*n*-6 for incorporation into the phospholipid compartment (Figure 4A), although there was no net change in the distribution of the fatty acid between compartments (Figure 4B). This lack of a difference between groups in the distribution of tracer in the total brain phospholipid pool may reflect the very large distribution of tracer in the phospholipid compartment ($\sim$90%), suggesting H-FABP has a lesser role in targeting of 20:4*n*-6 relative to the ability to influence movement of 20:4*n*-6 from the plasma compartment into the brain. In heart, H-FABP expression is more important in directing 16:0 into metabolic compartments and has very little effect on directing 20:4*n*-6 into these same compartments, despite a greater impact on heart 20:4*n*-6 incorporation (*13*). Thus, H-FABP appears to have a similar role in brain 20:4*n*-6 incorporation as it does in heart, although in brain there was no significant effect on 16:0 incorporation.

Sterol carrier protein-2 (SCP-2) is a ubiquitously distributed protein that is expressed in the brain (*51*, *52*). When expressed in cells, SCP-2 stimulates cholesterol uptake and trafficking (*53*, *54*) as well as stimulating fatty acid uptake and modulation of phospholipid acyl chain composition (*55*, *56*). Because SCP-2 comprises $\sim$0.08% of the total brain cytosolic protein (*51*) and displays a broad range of ligand binding, including a high affinity for both polyunsaturated fatty acids and saturated fatty acids (*57*), this protein may have an important role in brain saturated fatty acid uptake. In contrast, H-FABP may influence brain 20:4*n*-6 uptake, while SCP-2 may influence saturated fatty acid uptake. While it is unlikely that the level of expression of SCP-2 is increased in the brains of gene-ablated mice, we did not assess this point. Nonetheless, the lack of an effect on brain 16:0 uptake in the H-FABP deficient mice may be the result of SCP-2-mediated uptake of the saturated fatty acids into brain, whereas in the heart, H-FABP is critical for the uptake and trafficking of both 16:0 and 20:4*n*-6 (*13*).

FABP expression can influence fatty acid targeting within individual phospholipid classes (*13*, *45*, *47*). In H-FABP gene-ablated mouse hearts, despite the lack of altering targeting of 20:4*n*-6 to the total phospholipid pool, H-FABP expression did impact targeting within the individual phospholipid classes (*13*). Similarly, in brain H-FABP gene deletion inhibited the incorporation of 20:4*n*-6 into ChoGpl (Table 1), a lipid pool that is utilized by both phospholipase D- and phospholipase A_2-mediated signaling mechanisms (*58*−*71*). Hence, the decreased targeting of 20:4*n*-6 to the ChoGpl in gene-ablated mice may impact downstream signaling mechanisms in the brain due to a reduction in the extent of targeting of newly taken up 20:4*n*-6 to this pool. This may have an important role in diverse mechanisms such as the response to neuroinflammation to long-term potentiation in the hippocampus (*58*, *59*, *72*−*74*), a site where H-FABP is strongly expressed (*14*).

We examined the ability of H-FABP to target 20:4*n*-6 to the plasmalogen subclasses of ChoGpl and EtnGpl, because plasmalogens are phospholipids in which 20:4*n*-6 is concentrated (*75*, *76*) and because plasmalogens turn over rapidly in the brain (*29*). We did not find any alteration in incorporation of or targeting of 20:4*n*-6 to the plasmalogens. Further, our results demonstrate that the only phospholipid with an decrease in the level of incorporation was the phosphatidylcholine fraction of the ChoGpl. We recently demonstrated a similar lack of altered incorporation and targeting of 20:4*n*-6 to the heart plasmalogen pools (*13*), despite the fact that these pools are used for lipid-mediated signal transduction in the heart via a plasmalogen-selective phospholipase A_2 (*77*−*80*).

Because FABP expression is associated with increased phospholipid mass in cell culture systems (*20*) as well as associated with improved PtdOH biosynthesis in vitro (*22*−*24*), we analyzed brain steady-state lipid mass from wild-type and gene-ablated mice. Similar to what has been previously reported in other systems (*20*, *21*), H-FABP gene deletion decreased total phospholipid mass and the mass of individual choline-containing phospholipids (Table 2). However, consistent with what was observed in hearts from these mice (*13*), there was an increase in PtdOH and PtdGro mass, two precursors of phospholipid biosynthesis. The accumulation of these precursors, especially that of PtdOH as its synthesis is stimulated in vitro by FABP (*22*−*24*), appears to suggest an upregulation of phospholipid biosynthesis in the absence of H-FABP. However, a plausable alternative explanation is that there is an accumulation of these precursors due to a reduction in the level of ChoGpl biosynthesis via movement of PtdOH through the Kennedy pathway, which is the major pathway for the de novo synthesis of ChoGpl in brain (*81*, *82*).

Brain plasmalogen mass was also affected by H-FABP expression. The mass of PlsEtn was only reduced 13% in the absence of H-FABP; however, the mass of PlsCho was reduced 57% (Table 3). The difference in magnitude between the reduction in PlsCho and PlsEtn more than likely reflects the dilution of the active pool of gray matter PlsEtn by that found in myelin. We have previously reported that only gray matter pools of PlsEtn and PlsCho have a rapid rate of turnover (*29*), consistent with this hypothesis. In addition, 24 h following intracerebral injection of labeled 20:4*n*-6, the highest specific activity was in PlsCho, greater than that in PtdIns, PakCho, or PtdCho (*83*, *84*), further supporting the supposition that the PlsCho pool is rapidly turning over. Alternatively, our results suggest that the replacement of PlsCho in the absence of H-FABP, by its direct and only precursor PlsEtn, may be limited (*29*). This point is substantiated by the very large shift in the PlsEtn:PlsCho ratio, but once again this shift in the ratio may be influenced by the less metabolically active pool of PlsEtn in the white matter. In heart, H-FABP appears to be more important in maintaining the PlsEtn mass rather than that of PlsCho, because only the PlsEtn mass is significantly reduced (31%) by H-FABP gene ablation (*13*). Further, in heart, the PlsEtn:

PlsCho ratio was slightly decreased, suggesting a greater movement of PlsEtn into the PlsCho pool, perhaps to maintain the integrity of the PlsCho pool that is used in signaling (*77*−*80*). Both I-FABP expression and L-FABP expression enhance the plasmalogen mass in L-cell fibroblasts (*20*), consistent with what was observed in vivo. Although plasmalogens are only putative lipid signaling molecules in the brain (*29*, *83*−*86*), their rapid turnover with half-lives on the order of 15−30 min (*29*) suggests that these molecules coupled with neural signaling mechanisms, whether that be vesicular fusion events or direct receptor-mediated turnover as demonstrated in the heart (*77*−*80*). Hence, a decreased plasmalogen mass and potentially altered metabolism suggest a role for H-FABP in maintaining levels of this putative signaling molecule in the brain.

Because H-FABP gene ablation decreased the levels of 20:4*n*-6 with replacement by 22:6*n*-3 in the heart (*13*), we measured the phospholipid acyl chain composition in ChoGpl, EtnGpl, PtdSer, and PtdIns. In brain, there was a limited impact of H-FABP gene deletion on 20:4*n*-6 mass, and this was limited to a 25% reduction in the PtdIns 20:4*n*-6 level (Table 4). However, in each of the major phospholipid classes, there was a significant reduction in the level of total *n*-6 fatty acids, consistent with the preference of H-FABP for the *n*-6 fatty acid family (*9*). As in heart, brain PtdIns 20:4*n*-6 was replaced with more 22:6*n*-3. In EtnGpl and PtdIns, there was an increase in the level of monounsaturated fatty acids, attributed primarily to an increase in the level of oleic acid. Expression of I- and L-FABP affected phospholipid acyl chain composition in L-cell fibroblasts, with a general trend being an increase in the degree of unsaturation as well as an increase in 20:4*n*-6 and 22:6*n*-3 levels (*20*). Our results are consistent with those observed elsewhere, and suggest that in brain H-FABP has a significant role in maintaining the acyl chain composition of brain PtdIns.

In summary, H-FABP gene-ablation differentially decreased brain fatty acid incorporation, as demonstrated by a decrease in the level of incorporation of 20:4*n*-6 in the absence of altered 16:0 incorporation. Targeting of 20:4*n*-6 to lipid compartments was limited to reduced targeting to ChoGpl, a key phospholipid involved in ER lipid-mediated signaling 20:4*n*-6 release. Further, steady-state *n*-6 fatty acid levels were depressed in each of the major phospholipid classes, and there was a 25% reduction in 20:4*n*-6 levels in PtdIns, suggesting that H-FABP plays a role in maintaining these levels. In addition, steady-state phospholipid mass was also altered, including a reduction in ChoGpl and CerPCho mass as well as a marked reduction in the mass of the plasmalogens. Collectively, these results demonstrate a role for H-FABP in brain 20:4*n*-6 incorporation, maintenance of phospholipid *n*-6 fatty acid levels, and maintenance of steady-state phospholipid mass. Because H-FABP expression in brain is thought to be limited to neurons (*14*), there is a potential impact of these changes on neuronal lipid-mediated signal transduction. Further, these measurements were taken in the intact brain in which neurons comprise roughly 10% of the cells and where H-FABP comprises ~0.01% of the total cytosolic protein (*6*); thus, the magnitudes of the changes reported herein are quite significant. More importantly, these data indicate that the brain has selective processes for the incorporation and disposition of fatty acids into stable lipid compartments that are protein-mediated.

ACKNOWLEDGMENT

We thank Dr. Carole Haselton for her critical review of the manuscript and her excellent surgical and technical work and Mr. Will A. Coumans for his help with mice breeding and genotyping. We thank Cindy Murphy for typed preparation of the manuscript. We thank Drs. Othman Gribi, Thad Rosenberger, and Saobo Lei for their helpful comments.

REFERENCES

1. Binas, B., Danneberg, H., McWhir, J., Mullins, L., and Clark, A. J. (1999) Requirement for the heart-type fatty acid binding protein in cardiac fatty acid utilization, *FASEB J. 13*, 805−812.
2. Schaap, F. G., Binas, B., Danneberg, H., van der Vusse, G. J., and Glatz, J. F. C. (1999) Impaired long-chain fatty acid utilization by cardiac myocytes isolated from mice lacking the heart-type fatty acid binding protein gene, *Circ. Res. 85*, 329−337.
3. Zschiesche, W., Kleine, A. H., Spitzer, E., Veerkamp, J. H., and Glatz, J. F. C. (1995) Histochemical localization of heart-type fatty-acid binding protein in human and murine tissues, *Histochemistry 103*, 147−156.
4. Glatz, J. F. C., and van der Vusse, G. (1989) Intracellular transport of lipids, *Mol. Cell. Biochem. 88*, 37−44.
5. Pu, L., Annan, R. S., Carr, S. A., Frolov, A., Wood, W. G., Spener, F., and Schroeder, F. (1999) Isolation and identification of a mouse brain protein recognized by antisera to heart fatty acid-binding protein, *Lipids 34*, 363−373.
6. Myers-Payne, S., Hubbell, T., Pu, L., Schütgens, F., Börchers, T., Wood, W. G., Spener, F., and Schroeder, F. (1996) Isolation and characterization of two fatty acid binding proteins from mouse brain, *J. Neurochem. 66*, 1648−1656.
7. Qian, Q., Kuo, L., Yu, Y.-T., and Rottman, J. N. (1999) A concise promoter region of the heart fatty acid-binding protein gene dictates tissue-appropriate expression, *Circ. Res. 84*, 276−289.
8. Kim, H.-K., and Storch, J. (1992) Mechanism of free fatty acid transfer from rat heart fatty acid-binding protein to phospholipid membranes, *J. Biol. Chem. 267*, 20051−20056.
9. Hanhoff, T., Lucke, C., and Spener, F. (2002) Insights into binding of fatty acids by fatty acid binding proteins, *Mol. Cell. Biochem. 239*, 45−54.
10. Widstrom, R. L., Norris, A. W., Van Der Veer, J., and Spector, A. A. (2003) Fatty acid-binding proteins inhibit hydration of epoxyeicosatrienoic acids by soluble epoxide hydrolase, *Biochemistry 42*, 11762−11767.
11. Pu, L., Igbavboa, U., Wood, W. G., Roths, J. B., Kier, A. B., Spener, F., and Schroeder, F. (1999) Expression of fatty acid binding proteins is altered in aged mouse brain, *Mol. Cell. Biochem. 198*, 69−78.
12. Cheon, M. S., Kim, S. H., Fountoulakis, M., and Lubec, G. (2003) Heart type fatty acid binding protein (H-FABP) is decreased in brains of patients with Down syndrome and Alzheimer's disease, *J. Neural Transm., Suppl. 67*, 225−234.
13. Murphy, E. J., Barcelo-Coblijn, G., Binas, B., and Glatz, J. F. (2004) Heart fatty acid uptake is decreased in heart-fatty acid binding protein gene-ablated mice, *J. Biol. Chem. 279*, 34481−34488.
14. Owada, Y., and Kondo, H. (2003) Fatty acid binding protein of the brain, in *Cellular Proteins and Their Fatty Acids in Health and Disease* (Duttaroy, A. K., and Spener, F., Eds.) pp 253−265, Wiley-VCH, Weinheim, Germany.
15. Owada, Y., Yoshimoto, T., and Kondo, H. (1996) Spatio-temporally differential expression of genes for three members of fatty acid-binding proteins in developing and mature rat brains, *J. Chem. Neuroanat. 12*, 113−122.
16. Kurtz, A., Zimmer, A., Schnütgen, F., Brüning, G., Spener, F., and Müller, T. (1994) The expression pattern of a novel gene encoding brain-fatty acid binding protein correlates with neuronal and glial cell development, *Development 120*, 2637−2649.
17. Feng, L., Hatten, M. E., and Heintz, N. (1994) Brain lipid-binding protein (BLBP): A novel signaling system in the developing mammalian CNS, *Neuron 12*, 895−908.
18. Galarza De Bo, E. R., Atlasovich, F. M., Ermacora, M. R., Torea, J. H., Pasquini, J. M., Santome, J. A., and Soto, E. F. (1992) Rat brain fatty acid-binding protein during development, *Neurochem. Int. 21*, 237−241.

19. Sellner, P. A., Chu, W., Glatz, J. F. C., and Berman, N. E. J. (1995) Developmental role of fatty acid-binding proteins in mouse brain, *Dev. Brain Res. 89*, 33−46.
20. Murphy, E. J., Prows, D., Stiles, T., and Schroeder, F. (2000) Phospholipid and phospholipid fatty acid composition of L-cell fibroblast: Effect of intestinal and liver fatty acid binding protein, *Lipids 35*, 729−738.
21. Jolly, C. A., and Murphy, E. J. (2002) Role of FABP in cellular phospholipid metabolism, in *Cellular Proteins and Their Fatty Acids in Health and Disease* (Duttaroy, A. K., and Spener, F., Eds.) pp 327−342, Willey-VCH, Weinheim, Germany.
22. Jolly, C. A., Wilton, D. C., and Schroeder, F. (2000) Microsomal fatty acyl-CoA transacylation and hydrolysis: Fatty acyl-CoA species dependent modulation by liver fatty acyl-CoA binding proteins, *Biochim. Biophys. Acta 1483*, 185−197.
23. Jolly, C. A., Murphy, E. J., and Schroeder, F. (1998) Differential influence of rat liver fatty acid binding protein isoforms on phospholipid fatty acid composition: Phosphatidic acid biosynthesis and phospholipid fatty acid remodeling, *Biochim. Biophys. Acta 1390*, 258−268.
24. Jolly, C. A., Hubbell, T., Behnke, W. D., and Schroeder, F. (1997) Fatty acid binding protein: Stimulation of microsomal phosphatidic acid formation, *Arch. Biochem. Biophys. 341*, 112−121.
25. Freed, L. M., Wakabayashi, S., Bell, J. M., and Rapoport, S. I. (1994) Effect of inhibition of β-oxidation on incorporation of [U-^{14}C]palmitate and [1-^{14}C]arachidonate into brain lipids, *Brain Res. 645*, 41−48.
26. Folch, J., Lees, M., and Sloan Stanley, G. H. (1957) A simple method for the isolation and purification of total lipides from animal tissues, *J. Biol. Chem. 226*, 497−509.
27. Smith, B. S. (1970) A comparison of ^{125}I and ^{51}Cr for measurement of total blood volume and residual blood content of tissues in the rat: Evidence for accumulation of ^{51}Cr by tissues, *Clin. Chim. Acta 27*, 105−108.
28. Rosenberger, T. A., Villacreses, N. E., Contreras, M. A., Bonventre, J. V., and Rapoport, S. I. (2003) Brain lipid metabolism in the cPLA$_2$ knockout mouse, *J. Lipid Res. 44*, 109−117.
29. Rosenberger, T. A., Oki, J., Purdon, A. D., Rapoport, S. I., and Murphy, E. J. (2002) Rapid synthesis and turnover of brain microsomal ether phospholipids in the adult rat, *J. Lipid Res. 43*, 59−68.
30. Radin, N. S. (1988) Lipid extraction, in *Neuromethods 7: Lipids and Related Compounds* (Boulton, A. A., Baker, G. B., and Horrocks, L. A., Eds.) pp 1−62, Humana Press, Clifton, NJ.
31. Marcheselli, V. L., Scott, B. L., Reddy, T. S., and Bazan, N. G. (1988) Quantitative analysis of acyl group composition of brain phospholipids, neutral lipids, and free fatty acids, in *Neuromethods 7: Lipids and Related Compounds* (Boulton, A. A., Baker, G. B., and Horrocks, L. A., Eds.) pp 83−110, Humana Press, Clifton, NJ.
32. Rouser, G., Siakotos, A., and Fleischer, S. (1969) Quantitative analysis of phospholipids by thin-layer chromatography and phosphorus analysis of spots, *Lipids 1*, 85−86.
33. Hara, A., and Radin, N. S. (1978) Lipid extraction of tissues with a low-toxicity solvent, *Anal. Biochem. 90*, 420−426.
34. Dugan, L. L., Demediuk, P., Pendley, C. E., II, and Horrocks, L. A. (1986) Separation of phospholipids by high-pressure liquid chromatography: All major classes including ethanolamine and choline plasmalogens, and most minor classes, including lysophosphatidylethanolamine, *J. Chromatogr. 378*, 317−327.
35. Murphy, E. J., Stephens, R., Jurkowitz-Alexander, M., and Horrocks, L. A. (1993) Acidic hydrolysis of plasmalogens followed by high-performance liquid chromatography, *Lipids 28*, 565−568.
36. Brockerhoff, H. (1975) Determination of the positional distribution of fatty acids in glycerolipids, *Methods Enzymol. 35*, 315−325.
37. Glatz, J. F. C., Luiken, J. J. F. P., and Bonen, A. (2001) Involvement of membrane-associated proteins in the acute regulation of cellular fatty acid uptake, *J. Mol. Neurosci. 16*, 123−132.
38. Coburn, C. T., Hajri, T., Ibrahimi, A., and Abumrad, N. N. (2001) Role of CD36 in membrane transport and utilization of long-chain fatty acids by different tissues, *J. Mol. Neurosci. 16*, 117−121.
39. Herrmann, T., Buchkremer, F., Gosch, I., Hall, A. M., Bernlohr, D. R., and Stremmel, W. (2001) Mouse fatty acid transport protein 4 (FATP-4): Characterization of the gene and functional assessment as a very long chain acyl-CoA synthetase, *Gene 270*, 31−40.
40. Coort, S. L., Willems, J., Coumans, W. A., van der Vusse, G. J., Bonen, A., Glatz, J. F., and Luiken, J. J. (2002) Sulfo-N-succinimidyl esters of long chain fatty acids specifically inhibit fatty acid translocasa (FAT/CD36)-mediated cellular fatty acid uptake, *Mol. Cell. Biochem. 239*, 213−219.
41. Luiken, J. J., Coort, S. L., Koonen, D. P., van der Horst, D. J., Bonen, A., Zorzano, A., and Glatz, J. F. (2004) Regulation of cardiac long-chain fatty acid and glucose uptake by translocation of substrate transporters, *Pfluegers Arch. 448*, 1−15.
42. Utsunomiya, A., Owada, Y., Yoshimoto, T., and Kondo, H. (1997) Localization of mRNA for fatty acid transport protein in developing and mature brain of rats, *Brain Res. Mol. Brain Res. 46*, 217−222.
43. Hertzel, A. V., Bennaars-Eiden, A., and Bernlohr, D. A. (2002) Increased lipolysis in transgenic animals overexpressing the epithelial fatty acid binding protein in adipose cells, *J. Lipid Res. 43*, 2105−2111.
44. Kandel, E. R. (1991) in *Principles of Neural Science* (Kandel, E. R., Schwartz, J. H., and Jessel, T. M., Eds.) pp 18−32, Elsevier, New York.
45. Murphy, E. J., Prows, D. R., Jefferson, J. R., and Schroeder, F. (1996) Liver fatty acid binding protein expression in transfected fibroblasts stimulates fatty acid uptake and metabolism, *Biochim. Biophys. Acta 1301*, 191−196.
46. Prows, D. R., Murphy, E. J., and Schroeder, F. (1995) Intestinal and liver fatty acid binding proteins differentially affect fatty acid uptake and esterification in L-cells, *Lipids 30*, 907−910.
47. Prows, D. R., Murphy, E. J., Moncecchi, D., and Schroeder, F. (1996) Intestinal fatty acid-binding protein expression stimulates fibroblast fatty acid esterification, *Chem. Phys. Lipids 84*, 47−56.
48. Murphy, E. J. (1998) L-FABP and L-FABP expression increases NBD-stearate uptake and cytoplasmic diffusion in L cells, *Am. J. Physiol. 275*, G244−G249.
49. Gnaedinger, J. M., Miller, J. C., Latker, C. H., and Rapoport, S. I. (1988) Cerebral metabolism of plasma [^{14}C]palmitate in awake adult rat: Subcellular localization, *Neurochem. Res. 13*, 21−29.
50. Miller, J. C., Gnaedinger, J. M., and Rapoport, S. I. (1987) Utilization of plasma fatty acid in rat brain: Distribution of [^{14}C]-palmitate between oxidative and synthetic pathways, *J. Neurochem. 49*, 1507−1514.
51. Myers-Payne, S. C., Fontaine, R. N., Loeffler, A., Pu, L., Rao, A. M., Kier, A. B., Wood, W. G., and Schroeder, F. (1996) Effects of chronic consumption on sterol transfer proteins in mouse brain, *J. Neurochem. 66*, 313−320.
52. Gallegos, A. M., Atshaves, B. P., Storey, S. M., Starodub, O., Petrescu, A. D., Huang, H., McIntosh, A. L., Martin, G. G., Chao, H., Kier, A. B., and Schroeder, F. (2001) Gene structure, intracellular localization, and functional roles of sterol carrier protein-2, *Prog. Lipid Res. 40*, 498−563.
53. Moncecchi, D., Murphy, E. J., Prows, D. R., and Schroeder, F. (1996) Sterol carrier protein-2 expression in mouse L-cell fibroblasts alters cholesterol uptake, *Biochim. Biophys. Acta 1302*, 110−116.
54. Murphy, E. J., and Schroeder, F. (1997) Sterol carrier protein-2 mediated cholesterol esterification in transfected L-cell fibroblasts, *Biochim. Biophys. Acta 1345*, 283−292.
55. Murphy, E. J., Stiles, T., and Schroeder, F. (2000) Sterol carrier protein-2 expression alters phospholipid content and fatty acyl composition in L-cell fibroblasts, *J. Lipid Res. 41*, 788−796.
56. Murphy, E. J. (2002) Sterol carrier protein-2: Not just for cholesterol any more, *Mol. Cell. Biochem. 239*, 87−93.
57. Frolov, A., Miller, K., Billheimer, J. T., Cho, T. H., and Schroeder, F. (1997) Lipid specificity and location of the sterol carrier protein-2 fatty acid-binding site: A fluorescence displacement and energy transfer study, *Lipids 32*, 1201−1209.
58. Massicotte, G., Oliver, M. W., Lynch, G., and Baudry, M. (1990) Effect of bromophenacyl bromide, a phospholipase A$_2$ inhibitor, on the induction and maintenance of LTP in hippocampal slices, *Brain Res. 537*, 49−53.
59. Massicotte, G., Vanderklish, P., Lynch, G., and Baudry, M. (1991) Modulation of a DL-α-amino-3-hydroxy-5-methyl-4-isoxazolepropionic acid/quisqualate receptors by phospholipase A$_2$: A necessary step in long-term potentiation, *Proc. Natl. Acad. Sci. U.S.A. 88*, 1893−1897.
60. Lee, C., Kim, S. R., Chung, J. K., Frohman, M. A., Kilimann, M. W., and Rhee, S. G. (2000) Inhibition of phospholipase D by amphiphysins, *J. Biol. Chem. 275*, 18751−18758.
61. Klein, J., Chalifa, V., Liscovitch, M., and Löffelholz, K. (1995) Role of phospholipase D activation in nervous system physiology and pathophysiology, *J. Neurochem. 65*, 1445−1455.

62. Löffelholz, K. (1989) Receptor regulation of choline phospholipid hydrolysis: A novel source of diacylglycerol and phosphatidic acid, *Biochem. Pharmacol. 38*, 1543−1549.
63. Hung, A. C., and Sun, S. H. (2002) The $P2X_7$ receptor-mediated phospholipase D activation is regulated by both PKC-dependent and PKC-independent pathways in a rat brain-derived type-2 astrocyte cell line, RBA-2, *Cell. Signalling 14*, 83−92.
64. Watanabe, H., Yamazaki, M., Miyazaki, H., Arikawa, C., Itoh, K., Sasaki, T., Maehama, T., Frohman, M. A., and Kanaho, Y. (2004) Phospholipase D2 functions as a downstream signaling molecule of MAP kinase pathway in L1-stimulated neurite outgrowth of cerebellar granule neurons, *J. Neurochem. 89*, 142−151.
65. Klapisz, E., Ziari, M., Wendum, D., Koumanov, K., Brachet-Ducos, C., Olivier, J.-L., Béréziat, G., Trugnan, G., and Masliah, J. (1999) N-Terminal and C-terminal plasma membrane anchoring modulate differently agonist-induced activation of cytosolic phospholipase A_2, *Eur. J. Biochem. 265*, 957−966.
66. Paintlia, A. S., Gilg, A. G., Khan, M., Signh, A. K., Barbosa, E., and Singh, I. (2003) Correlation of very long chain fatty acid accumulation and inflammatory disease progression in childhood X-ALD implications for potential therapies, *Neurobiol. Dis. 14*, 425−439.
67. Arai, K., Ikegaya, Y., Nakatani, Y., Kudo, I., Nishiyama, N., and Matsuki, N. (2001) Phospholipase A_2 mediates ischemic injury in the hippocampus: A regional difference of neuronal vulnerability, *Eur. J. Neurosci. 13*, 2319−2323.
68. Bosetti, F., and Weerasinghe, G. R. (2003) The expression of brain cyclooxygenase-2 is down-regulated in the cytosolic phospholipase A_2 knockout mouse, *J. Neurochem. 87*, 1471−1477.
69. Rodriguez de Turco, E. B., Jackson, F. R., DeCoster, M. A., Kolko, M., and Bazan, N. G. (2002) Glutamate signalling and secretory phospholipase A_2 modulate the release of arachidonic acid from neuronal membranes, *J. Neurosci. Res. 68*, 558−567.
70. St-Gelais, F., Menard, C., Congar, P., Trudeau, L. E., and Massicotte, G. (2004) Postsynaptic injection of calcium-independent phospholipase A_2 inhibitors selectively increases AMPA receptor-mediated synaptic transmission, *Hippocampus 14*, 319−325.
71. Farooqui, A. A., Antony, P., Ong, W.-Y., Horrocks, L. A., and Freysz, L. (2004) Retinoic acid-mediated phospholipase A_2 signaling in the nucleus, *Brain Res. Rev. 45*, 179−195.
72. Clements, M. P., Bliss, T. V. P., and Lynch, M. A. (1991) Increase in arachidonic acid concentration in a postsynaptic membrane fraction following the induction of long-term potentiation in the dentate gyrus, *Neuroscience 45*, 379−389.
73. Williams, J. H., Errington, M. L., Lynch, M. A., and Bliss, T. V. P. (1989) Arachidonic acid induces a long-term activity-dependent enhancement of synaptic transmission in the hippocampus, *Nature 341*, 739−742.
74. Rosenberger, T. A., Villacreses, N. E., Hovda, J. T., Boestti, F., Weerasinghe, G., Wine, R. N., Harry, G. J., and Rapoport, S. I. (2004) Rat brain arachidonic acid metabolism is increased by a 6-day intracerebral ventricular infusion of bacterial lipopolysaccharide, *J. Neurochem. 88*, 1168−1178.
75. Gross, R. W. (1984) High plasmalogen and arachidonic acid content of canine myocardial sarcolemma: A fast atom bombardment mass spectroscopic and gas chromatography−mass spectroscopic characterization, *Biochemistry 23*, 158−165.
76. Gross, R. W. (1985) Identification of plasmalogen as the major phospholipid constituent of cardiac sarcoplasmic reticulum, *Biochemistry 24*, 1662−1668.
77. Ford, D. A., Hazen, S. L., Saffitz, J. E., and Gross, R. W. (1991) The rapid and reversible activation of a calcium-independent plasmalogen-selective phospholipase A_2 during myocardial ischemia, *J. Clin. Invest. 88*, 331−335.
78. McHowat, J., and Liu, S. (1997) Interleukin-1b stimulates phospholipase A_2 activity in adult rat ventricular myocytes, *Am. J. Physiol. 272*, C450−C456.
79. McHowat, J., and Creer, M. H. (2000) Selective plasmalogen substrate utilization by thrombin-stimulated Ca^{2+}-independent PLA_2 in cardiomyocytes, *Am. J. Physiol. 278*, H1933−H1940.
80. McHowat, J., and Creer, M. H. (2001) Comparative roles of phospholipase A_2 isoforms in cardiovascular pathophysiology, *Cardiovasc. Toxicol. 1*, 253−265.
81. Murphy, E. J., and Horrocks, L. A. (1990) Mechanisms of action of CDPcholine and CDPethanolamine on fatty acid release during ischemia of brain, in *Lipid Mediators in Ischemic Brain Damage and Experimental Epilepsy* (Bazan, N. G., Karger, S., and Basel, A. G., Eds.) pp 67−84, Karger Press, Basel, Switzerland.
82. McMaster, C. R., and Bell, R. M. (1997) CDP-choline:1,2-diacylglycerol cholinephosphotransferase, *Biochim. Biophys. Acta 1348*, 100−110.
83. Horrocks, L. A., Yeo, Y. K., Harder, H. W., Mozzi, R., and Goracci, G. (1986) Choline plasmalogens, glycerophospholipid methylation, and receptor-mediated activation of adenylate cyclase, in *Advances in Cyclic Nucleotide Protein Phosphorylation Research* (Greengard, P., and Robinson, G. A., Eds.) Vol. 20, pp 263−292, Raven Press, New York.
84. Horrocks, L. A., Harder, H. W., Mozzi, R., Goracci, G., Francescangeli, E., Porcellati, S., and Nenci, G. G. (1986) Receptor mediated degradation of choline plasmalogen and glycerophospholipid methylation: A new hypothesis, in *Enzymes of Lipid Metabolism* (Freysz, L., Dreyfus, H., Massarelli, R., and Gatt, S., Eds.) Vol. 2, pp 707−711, Plenum Press, New York.
85. Hirashima, Y., Mills, J. S., Yates, A. J., and Horrocks, L. A. (1990) Phospholipid A_2 activities with a plasmalogen substrate in brain and in neural tumor cells: A sensitive and specific assay using pyrenesulfonyl-labeled plasmenylethanolamine, *Biochim. Biophys. Acta 1047*, 35−40.
86. Hirashima, Y., Farooqui, A. A., Mills, J. S., and Horrocks, L. A. (1992) Identification and purification of calcium-independent phospholipase A_2 from bovine brain cytosol, *J. Neurochem. 59*, 708−714.

BI047292R